

# Pilot Symbol Assisted Hybrid Detection for OFDM-Based Spatial Multiplexing Systems

---

Yoon-Jae So, Hyoung-Goo Jeon, Young-Hwan You,  
Myung-Sun Baek, and Hyoung-Kyu Song

**In this paper, we provide a new detection scheme for a pilot symbol assisted interference nulling and cancellation operation to reduce unexpected effects owing to parallel transmission in orthogonal frequency division multiplexing (OFDM)-based spatial multiplexing systems. We have shown that the investigated OFDM vertical Bell laboratories layered space time (VBLAST) detection based on hybrid processing performs better than ordinary OFDM-VBLAST detections based on serial processing and parallel processing, respectively.**

**Keywords: OFDM, VBLAST, nulling, cancellation, parallel transmission.**

## I. Introduction

The goal of future wireless communication is to provide high quality wireless multimedia services; thus, high data rate communication must be transmitted reliably. Recent theoretic research has shown that multiple transmitting and receiving antenna systems can achieve enormous spectral efficiency. Various multiple-input multiple-output (MIMO) systems have been proposed to attain this available capacity [1], [2].

Orthogonal frequency division multiplexing (OFDM) is one of the most attractive multicarrier modulation schemes for high bandwidth efficiency and strong immunity to multi-path fading. Thus, multiple transmitting and receiving antennas can be used with OFDM to improve the communication capacity and quality of mobile wireless systems [3]-[6]. Among these algorithms, the OFDM-based Bell laboratories layered space-time (BLAST), with a number of transmitting and receiving antennas, increases the transmission rate efficiently using low multiplication operations [6]. Such algorithms could provide very high data-rate communication over wireless channels without increasing the total transmission power and bandwidth. Based on its knowledge of the matrix of propagation coefficients, the vertical-BLAST (VBLAST) detection scheme is often referred to as sequential nulling and cancellation. Recently, various detection methods for improving VBLAST systems have been proposed [7]-[9].

In this paper, we develop an efficient hybrid detection algorithm for the nulling vector and cancellation in VBLAST systems. The simulation results describe the effect of the pilot symbol assisted interference cancellation and hybrid detection in OFDM-based VBLAST systems, and the performance of the hybrid VBLAST detection algorithm is superior to that of

---

Manuscript received Dec. 14, 2003; revised Aug. 17, 2004.

This research was supported by University IT Research Center Project.

Yoon-Jae So (phone: +82 2 3408 3890, email: 99allaplus@hanmail.net), Young-Hwan You (email: yhyou@sejong.ac.kr), Myung-Sun Baek (email: sabzaloo@hanmail.net), and Hyoung-Kyu Song (email: songhk@sejong.ac.kr) are with the uT Communication Institute, Sejong University, Seoul, Korea.

Hyoung-Goo Jeon (email: hgjeon@dongeui.ac.kr) is with the Department of Information and Communications Engineering, Dongeui University, Busan, Korea.

ordinary VBLAST detection algorithms based on serial detection [2] and parallel detection [7].

This paper is organized as follows. In section II, the system description is presented, section III and IV explain pilot preamble structure and pilot symbol assisted channel separation, respectively. In sections V and VI, hybrid VBLAST detection and a modified nulling of the hybrid VBLAST detection algorithm are derived briefly. Finally, in section VII, simulation results and discussions are described.

## II. System Description

We consider OFDM-based VBLAST systems with  $N_t$  transmitting and  $N_r$  receiving antennas. The OFDM data sequence of the  $n$ -th transmitting antenna is represented as  $\mathbf{X}_n = [X_n(0) X_n(1) \cdots X_n(K-1)]^T$ , where  $X_n(l)$ ,  $n = 1, 2, \dots, N_t$  is the complex baseband signal of the  $l$ -th subcarrier, and  $K$  is the length of the OFDM data sequence. Because the symbols are transmitted from  $N_t$  transmitting antennas in parallel, the  $N_t \times K$  data sequence matrix is  $\mathbf{X} = [\mathbf{X}_1 \mathbf{X}_2 \cdots \mathbf{X}_{N_t}]^T$ .

A flat fading channel on each subcarrier and independent identically distributed fading among different subcarriers are assumed in our analysis. Also, we assume that the time variation of fading is negligible over a frame, which is estimated using the pilot preamble. The time delay and phase offset of each antenna are assumed to be known, i.e., tracked accurately. Therefore, the overall channel,  $\mathbf{H}$ , can be represented as an  $N_r \times N_t$  complex matrix, and the baseband received signal at the  $j$ -th receiving antenna is

$$r_j(l) = \sum_{i=1}^{N_t} h_{ji} X_i(l) + v_j(l), \quad (1)$$

where  $h_{ji}$  is the channel element with the  $i$ -th transmitting antenna and  $j$ -th receiving antenna and  $v_j(l)$  is zero-mean Gaussian noise with variance  $\sigma_v^2$ . The overall received signals can be represented as

$$\mathbf{R} = \mathbf{H}\mathbf{X} + \mathbf{V}. \quad (2)$$

where  $\mathbf{R}$  and  $\mathbf{V}$  are the  $N_r \times K$  matrices, respectively.

## III. Preamble Structure Using Pilot Symbol

We consider an OFDM system with  $K$  subcarriers that uses  $N_t$  transmitting and  $N_r$  receiving antennas. If we denote  $X_i(k)$  for frequency-domain index  $0 \leq k \leq K$  as a preamble pattern for the  $i$ -th transmitting antenna for  $1 \leq i \leq N_t$ ,  $x_i(n)$  is then the inverse fast Fourier transform output of the preamble

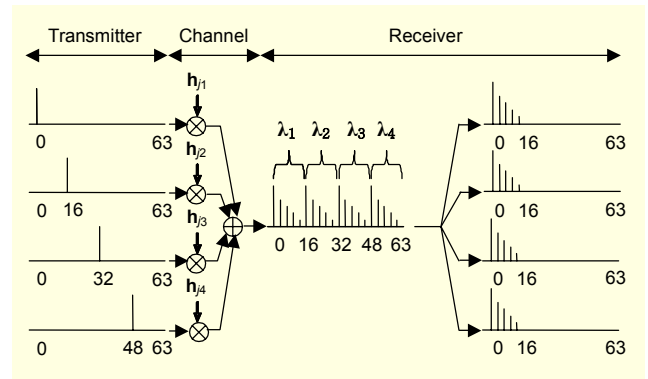


Fig. 1. Process of pilot symbol assisted channel separation in the case of  $K = 64$  and  $L = 16$ .

pattern for the first transmitting antenna denoted as  $X_1(k)$ . The relationship is derived as the following rule:

$$X_i(k) = \text{FFT}[x_i(n-n_i)], \quad (3)$$

where  $n$  is the time-domain index ( $0, 1, \dots, K-1$ ) of an OFDM symbol and  $n_i$  is any integer for time shifting in the  $i$ -th preamble pattern. If we denote  $x_i(n-n_i)$  as  $x_i(n)$ , the vector of preamble pattern  $\mathbf{x}_i$  for the  $i$ -th transmitting antenna is presented as follows:

$$\mathbf{x}_i = [x_i(0) x_i(1) \cdots x_i(K-1)]^T = [\underbrace{0 \cdots 0}_{n_i} 1 0 \cdots 0]^T. \quad (4)$$

For a given number of substantial subcarriers used in data modulation denoted by  $K$  and a channel response with a length of  $L$ , the maximum number of transmitting antennas  $N_t$  can be given by

$$N_t = \lfloor K/L \rfloor, \quad (5)$$

where  $\lfloor a \rfloor$  gives the largest integer not exceeding  $a$ , and  $L$  is the maximum number of channel paths between each pair of transmitting and receiving antennas. Considering (5), the time shift index for each  $N_t$  multiple transmitting antennas can be designed as

$$n_i = (i-1) \lfloor K/N_t \rfloor \quad \text{for } 1 \leq i \leq N_t. \quad (6)$$

When a design criterion of  $\lfloor K/N_t \rfloor \geq L$  is satisfied, orthogonality is still maintained even if encountered with a channel impulse response with a length of  $L$ , which is illustrated in Fig. 1. In this example, the number of transmitting antennas,  $N_t = 4$  from (5), and  $\mathbf{x}_i$ 's for  $1 \leq i \leq N_t$  are shown in Fig. 1. In the case of four transmitting antennas, from (3), the

preamble pattern in the frequency domain can be expressed as

$$\begin{aligned} \mathbf{X}_1 &= [1 \ 1 \ 1 \ 1 \ \cdots \ 1 \ 1 \ 1 \ 1]^T, \\ \mathbf{X}_2 &= [1 \ -j \ -1 \ j \ \cdots \ 1 \ -j \ -1 \ j]^T, \\ \mathbf{X}_3 &= [1 \ -1 \ 1 \ -1 \ \cdots \ 1 \ -1 \ 1 \ -1]^T, \\ \mathbf{X}_4 &= [1 \ j \ -1 \ -j \ \cdots \ 1 \ j \ -1 \ -j]^T. \end{aligned} \quad (7)$$

#### IV. Preamble Structure Using Pilot Symbol

For each transmitting antenna  $i$ , we assume that a transmitted OFDM symbol goes through a multi-path channel before reaching the  $j$ -th receiving antenna with the channel impulse response modeled by

$$\mathbf{h}_{ji} = [h_{ji}(0) \ h_{ji}(1) \ \cdots \ h_{ji}(L-1)]^T. \quad (8)$$

Then, the received time-domain samples of an OFDM symbol from receiver  $j$  can be expressed as

$$\mathbf{r}_j = \sum_{i=1}^{N_t} \mathbf{x}_i \otimes \mathbf{h}_{ji} + \mathbf{v}_j = \sum_{i=1}^{N_t} \mathbf{g}_{ji} + \mathbf{v}_j, \quad (9)$$

where  $\otimes$  represents  $K$ -point circular convolution,  $\mathbf{v}_j = [v_j(0) \ v_j(1) \ \cdots \ v_j(K-1)]^T$  are independent identically distributed additive white Gaussian noise (AWGN) samples with zero mean and a variance of  $\sigma_i^2$ , and  $\mathbf{g}_{ji}$  is the  $n_i$ -th cyclic shifted version of  $\mathbf{h}_{ji}$ , which is given by

$$\mathbf{g}_{ji} = [0 \ \cdots \ 0 \ \underbrace{h_{ji}(0) \ h_{ji}(1) \ \cdots \ h_{ji}(L-1)}_K \ 0 \ \cdots \ 0]^T. \quad (10)$$

As shown in Fig. 1, multiplying the received signal  $\mathbf{r}_j$  at the  $j$ -th receiving antenna with a rectangular window vector, which is defined as  $\boldsymbol{\lambda}$ , yields

$$\mathbf{y}_j = \boldsymbol{\lambda} \mathbf{r}_j = \mathbf{g}_j + \hat{\mathbf{v}}_j, \quad (11)$$

where  $\boldsymbol{\lambda} = [\lambda_1 \ \lambda_2 \ \cdots \ \lambda_{N_t}]^T$  with each element of a  $K \times K$  diagonal matrix is

$$\boldsymbol{\lambda}_i = \text{diag}[0 \ \cdots \ 0 \ \underbrace{1 \ \cdots \ 1}_{n_i} \ \cdots \ 0], \quad (12)$$

$\mathbf{g}_j = [\mathbf{g}_{j1} \ \mathbf{g}_{j2} \ \cdots \ \mathbf{g}_{jN_t}]$ , and  $\hat{\mathbf{v}}_j = [\mathbf{v}_{j1} \ \mathbf{v}_{j2} \ \cdots \ \mathbf{v}_{jN_t}]$  with each component expressed as

$$\mathbf{v}_{ji} = [0 \ \cdots \ 0 \ \underbrace{v_{ji}(n_i) \ \cdots \ v_{ji}(n_i + \lfloor K/N_t \rfloor - 1)}_{\lfloor K/N_t \rfloor} \ 0 \ \cdots \ 0]^T. \quad (13)$$

Then, as shown in Fig. 1, it removes the effect of  $\mathbf{x}_i$  by shifting  $\mathbf{g}_{ji}$  by  $\mathbf{n}_i$  on the left, and  $\mathbf{y}_j$  can be rewritten as

$$\mathbf{y}'_j = \mathbf{g}'_j + \hat{\mathbf{v}}'_j, \quad (14)$$

where  $\mathbf{g}'_j = [\mathbf{g}'_{j1} \ \mathbf{g}'_{j2} \ \cdots \ \mathbf{g}'_{jN_t}]^T$  with each component of  $K$ -dimensional vector  $\mathbf{g}'_{ji} = [h_{ji}(0) \ h_{ji}(1) \ \cdots \ h_{ji}(L-1) \ 0 \ \cdots \ 0]^T$  and  $\hat{\mathbf{v}}'_j = [\mathbf{v}'_{j1} \ \mathbf{v}'_{j2} \ \cdots \ \mathbf{v}'_{jN_t}]^T$ , with each component rewritten as  $\mathbf{v}'_{ji} = [v_{ji}(n_i) \ \cdots \ v_{ji}(n_i + \lfloor K/N_t \rfloor - 1) \ 0 \ \cdots \ 0]^T$ .

If we choose a normalization factor of the transmission power, the FFT output of the frequency-domain subcarriers can be formulated as

$$\mathbf{Y}'_j = \mathbf{F} \mathbf{y}'_j = \mathbf{H}_j + \hat{\mathbf{V}}_j, \quad (15)$$

where  $\mathbf{H}_j$  and  $\hat{\mathbf{V}}_j$  are the FFT output of  $\mathbf{g}'_j$  and  $\hat{\mathbf{v}}'_j$ , respectively, and  $\mathbf{F}$  is a  $K \times K$  FFT matrix given by

$$\mathbf{F} = \begin{pmatrix} W_K^{00} & W_K^{01} & \cdots & W_K^{0(K-1)} \\ W_K^{10} & W_K^{11} & \cdots & W_K^{1(K-1)} \\ \vdots & \vdots & \ddots & \vdots \\ W_K^{(K-1)0} & W_K^{(K-1)1} & \cdots & W_K^{(K-1)(K-1)} \end{pmatrix}, \quad (16)$$

with  $W_K^{nk} = \exp\{-j2\pi \frac{nk}{K}\} / \sqrt{K}$ . Therefore, channel  $\mathbf{H}_j$  can be estimated using a simple least square (LS) method, and the LS estimation of the channel impulse response is

$$\hat{\mathbf{H}}_{LS} = \mathbf{Y}'_j = \hat{\mathbf{H}}_j. \quad (17)$$

Furthermore, this can be easily extended to the linear minimum mean square error (LMMSE) estimator. In order to have the minimum amount of information necessary, the estimator assumes a priori knowledge of noise variance and channel covariance and is expressed as

$$\hat{\mathbf{H}}_{LMMSE} = \mathbf{R}_H \left( \mathbf{R}_H + \frac{1}{\text{SNR}} \mathbf{I} \right)^{-1} \hat{\mathbf{H}}_{LS}, \quad (18)$$

where  $\mathbf{R}_H = E[\mathbf{H}_j \mathbf{H}_j^H]$  is the auto-covariance matrix of  $\mathbf{H}_j$ , the superscript  $(\cdot)^H$  denotes the Hermitian transpose, and  $\mathbf{I}$  is the identity matrix.

Both estimators (17) and (18) have their merits and demerits. The complexity of the LMMSE estimator is larger than that of the LS estimator. For a high signal-to-noise ratio (SNR), the LS estimator is simple and adequate. The LMMSE channel estimator is better than the LS channel estimator because of its

higher ability for noise and interference suppression. However, when the SNR is high, and when co-channel interference is not present, the difference is not obvious.

### V. Hybrid VBLAST Detection

In this section, we will present techniques for signal detection, including hybrid detection for a nulling vector and cancellation. The detail operation of the hybrid VBLAST detection scheme is illustrated in Fig. 2. Initially, the antennas are ranked in decreasing order of the irrespective received signal power using the power ranking information extracted from the power ranking scheme.

The regenerated signals from the first antenna to the  $j$ -th antenna at the  $j$ -th stage at time  $l$  are subtracted from the delayed version of received signal  $r^0(l)$  as follows:

$$r^j(l) = r^0(l) - \sum_{k=1}^j \hat{r}_k^{j-1}(l), \quad (19)$$

where  $\hat{r}_k^{j-1}(l)$  is the regenerated signal of the  $k$ -th antenna from the  $(j-1)$ th stage. This replica is regenerated by using the estimated channel based on the pilot preamble.

Equation (19) is the interference-cancelled signal for the input of a nulling and regeneration unit of all the antennas at the  $j$ -th stage. In Fig. 3, the regenerated signal of the  $i$ -th antenna at the previous stage, denoted as  $\hat{r}_i^{j-1}(l)$ , is added to the interference cancelled signal, denoted as  $r^j(l)$ , in order to obtain the corresponding composite signal as follows:

$$\hat{r}_i^j(l) = r^0(l) - \sum_{\substack{k=1 \\ k \neq i}}^j \hat{r}_k^{j-1}(l) = r^j(l) + \hat{r}_i^{j-1}(l), \quad (20)$$

which is nulled by the corresponding antenna's nulling vector

and is forwarded to the decision block. Therefore, the nulling and regeneration unit in the hybrid scheme performs only the projection of the received signal of the corresponding antenna. Finally, the decision variable  $z_i^j$  is forwarded to the next stage for a cleaner regeneration when  $j < N_t$ . On the other hand, when  $j = N_t$ , the decision variable is forwarded to the final bit decision device.

As the delayed detection proceeds, the delayed version of the received signal is subtracted by all of the other antennas' signals except for the desired antenna's signal. This hybrid process is repeated until the cancellation stage reaches the maximum stage. In the original sequential VBLAST detection scheme, the received signal  $r^j(l)$  is subtracted by only one regenerated signal of the  $j$ -th antenna at every inter-stage. In the hybrid VBLAST detection scheme, however, it is subtracted by all regenerated signals from the first to the  $j$ -th antenna at every inter-stage.

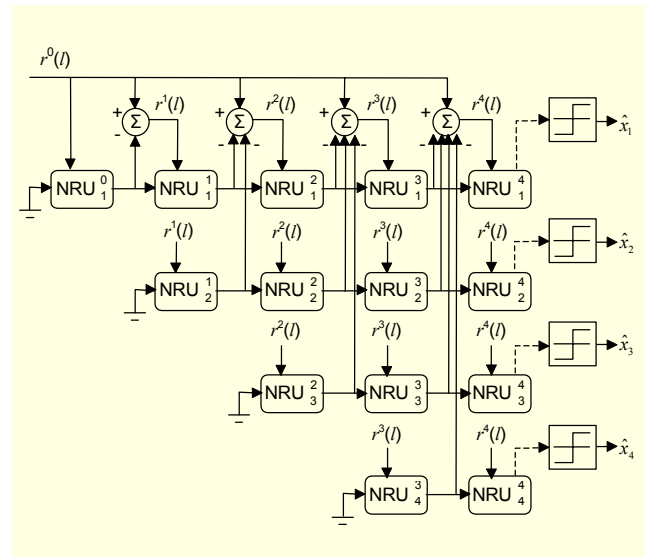


Fig. 2. The hybrid detection scheme for VBLAST system under  $N_t = 4$  and  $N_r = 4$ .

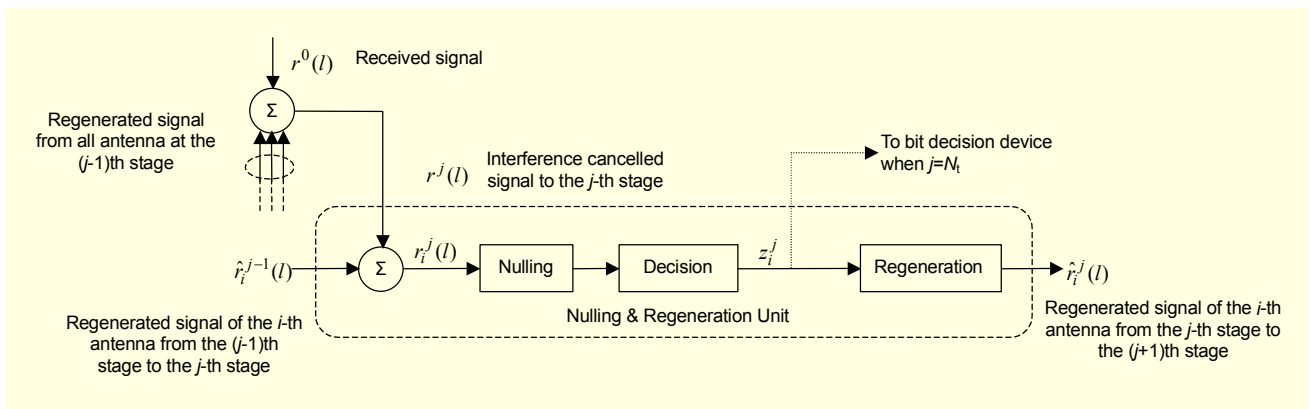


Fig. 3. The nulling and regeneration unit at the  $j$ -th stage of  $i$ -th antenna at time  $l$ .

## VI. Modified Nulling of the Hybrid VBLAST Detection

For the  $N_r \times 1$  vector of transmitted data symbols at time  $l$ , denoted as  $\mathbf{x} = [x_1(l) x_2(l) \cdots x_{N_t}(l)]^T$ , the corresponding received  $N_r \times 1$  vector is

$$\mathbf{r}^0 = \mathbf{H}\mathbf{x} + \mathbf{v}, \quad (21)$$

where  $\mathbf{H} = [\mathbf{h}_1 \mathbf{h}_2 \cdots \mathbf{h}_{N_t}]^T$  is a multi-path channel with each element of  $\mathbf{h}_n = [h_{n1} h_{n2} \cdots h_{nN_r}]$ , and  $\mathbf{v} = [v_1(l) v_2(l) \cdots v_{N_r}(l)]^T$  is the AWGN vector with variance  $\sigma_v^2$ .

We perform the sequential detection of the elements in  $\mathbf{x}$ . Note that we do not need to detect element  $x_i$  in the order of  $i = 1, 2, \dots, N_t$ . Therefore, the optimal ordering to minimize the detection error is founded. It turns out that we can obtain the optimal ordering by selecting the minimum-norm column of  $\mathbf{H}^\dagger$ , where  $(\cdot)^\dagger$  indicates a pseudo-inverse. Let the optimal detection ordering be  $[x_{k_1} x_{k_2} \cdots x_{k_{N_t}}]$ .

To detect the  $i$ -th element of  $\mathbf{x}$ ,  $x_{k_i}$ , we perform zero-forcing nulling. We find the minimum norm weight vector  $\mathbf{w}_{k_i}$  such that

$$\mathbf{w}_{k_i}^H \mathbf{h}_{k_i} = \delta_{k_i}, \quad (22)$$

where  $(\cdot)^H$  means the complex conjugate transpose. Weight vector  $\mathbf{w}_{k_i}$  can be obtained from the pseudo-inverse of  $\mathbf{H}$ , and using its estimator,  $\hat{\mathbf{H}}$ , we obtain the weight vector,

$$\hat{\mathbf{w}}_{k_i} = (\hat{\mathbf{G}}_i)_{k_i}^*, \quad (23)$$

where

$$\hat{\mathbf{G}}_{i+1} = \hat{\mathbf{H}}_{k_i-}^\dagger \quad (24)$$

and the notation  $\mathbf{H}_{k_i-}^\dagger$  denotes the matrix obtained by zeroing columns  $k_1, k_2, \dots, k_i$  of  $\mathbf{H}$ .

When the  $i$ -th symbol is detected, the received vector  $\mathbf{r}^j$  after cancelling  $x_{k_l}$ ,  $l = 0, 1, \dots, j-1$ , becomes

$$\mathbf{r}^j = \mathbf{r}^0 - \sum_{l=0}^{j-1} \hat{x}_{k_l} \hat{\mathbf{h}}_{k_l} + \mathbf{v}. \quad (25)$$

Assume that no detection error of  $x_{k_l}$  gives

$$\begin{aligned} \mathbf{r}^j &= \mathbf{H}\mathbf{x} - \sum_{l=0}^{j-1} x_{k_l} \hat{\mathbf{h}}_{k_l} + \mathbf{v} \\ &= \mathbf{H}_{k_i-} \mathbf{x}_{k_i-} - \sum_{l=0}^{j-1} x_{k_l} \mathbf{h}_{k_l} + \mathbf{v} \\ &= \hat{\mathbf{H}}_{k_i-} \mathbf{x}_{k_i-} - \Delta \mathbf{H}_{k_i-} \mathbf{x}_{k_i-} - \sum_{l=0}^{j-1} x_{k_l} \mathbf{h}_{k_l} + \mathbf{v}, \end{aligned} \quad (26)$$

where

$$\begin{aligned} \mathbf{x}_{k_i-} &= [x_{k_i} x_{k_{i+1}} \cdots x_{k_{N_t}}], \\ \hat{\mathbf{H}}_{k_i-} &= [\hat{\mathbf{h}}_{k_i} \hat{\mathbf{h}}_{k_{i+1}} \cdots \hat{\mathbf{h}}_{k_{N_t}}], \\ \Delta \mathbf{H}_{k_i-} &= [\Delta \mathbf{h}_{k_i} \Delta \mathbf{h}_{k_{i+1}} \cdots \Delta \mathbf{h}_{k_{N_t}}]. \end{aligned} \quad (27)$$

If  $\Delta \mathbf{H} = 0$ ,  $\hat{\mathbf{w}}_{k_i}$  in (23) is an optimal nulling vector. But in a real system, there is nonzero matrix  $\Delta \mathbf{H}$ , and  $\hat{\mathbf{w}}_{k_i}$  is not the optimal nulling vector. We derive hereafter the new nulling vector which minimizes the unexpected effect of the channel estimation error. Without loss of generality, the new nulling vector  $\bar{\mathbf{w}}_{k_i}$  is written as

$$\bar{\mathbf{w}}_{k_i} = \hat{\mathbf{w}}_{k_i} + \Delta \mathbf{w}_{k_i}, \quad (28)$$

where  $\Delta \mathbf{w}_{k_i}$  indicates the difference between original nulling vector  $\hat{\mathbf{w}}_{k_i}$  and new nulling vector  $\bar{\mathbf{w}}_{k_i}$ . With the new nulling vector, we obtain the new decision statistic, and the estimate of  $\hat{x}_{k_i}$  is as follows:

$$\hat{x}_{k_i} = Q(\bar{\mathbf{w}}_{k_i}^H \mathbf{r}_i^j), \quad (29)$$

where  $Q(\cdot)$  is the quantization operation appropriate to the constellation in use.

## VII. Simulation Results and Discussions

In this section, we evaluate the detection performances of both a perfect channel and LMMSE channel estimations for the various VBLAST detection schemes for a Rayleigh fading channel with a multi-path length of  $L = 16$ . The channel model is assumed to be an equal and exponential multi-path power delay profile.

In Fig. 4, the channel estimation is done by using the pilot preamble described, and the performance of the LMMSE estimator is measured using  $\text{MSE} = E[(\mathbf{H} - \hat{\mathbf{H}}_{\text{LMMSE}})^2]$ . This figure validates the effectiveness of the investigated preamble structure, which is designed based on the assumption that the length of the guard interval in both ETSI HIPERLAN/2 and IEEE802.11a standards is 16. In general, this means that time delay  $L$  (or, delay spread) is less than 16. So, multi-paths of 9 and 16 are corresponding to the optimum and worst cases, respectively. The worst case is a 1.5 dB degradation compared with the optimum case. As the propagation length of  $L$  exceeds the window size of 16, the MSE of the LMMSE estimator increases and the MSE performance of the exponential power delay profile is less decreased than that of the equal power delay profile. When the SNR is less than 30dB, fortunately, the MSE degradation in the

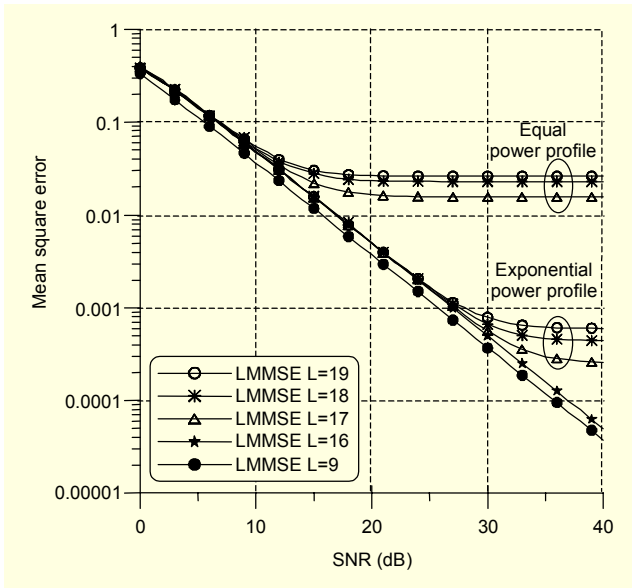


Fig. 4. MSE performance of LMMSE estimation for pilot preamble according to the type of delay profile with  $N_t = 4$  and  $N_r = 4$ .

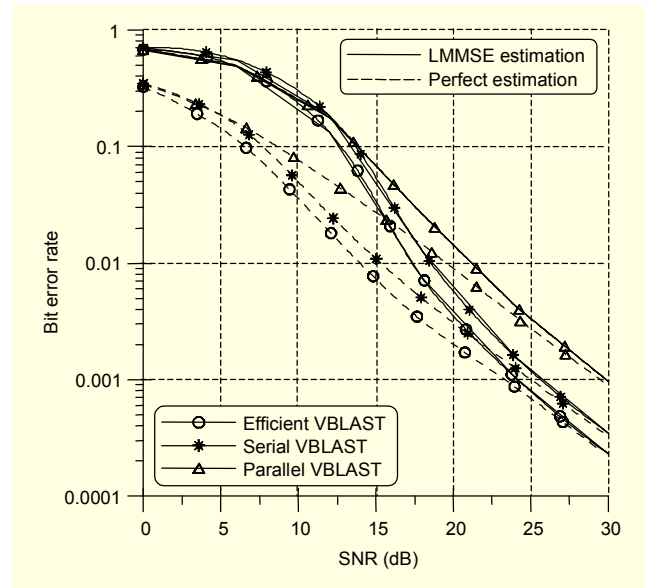


Fig. 6. BER performance of various OFDM-VBLAST detection schemes in the case of  $N_t=4$  and  $N_r=4$ .

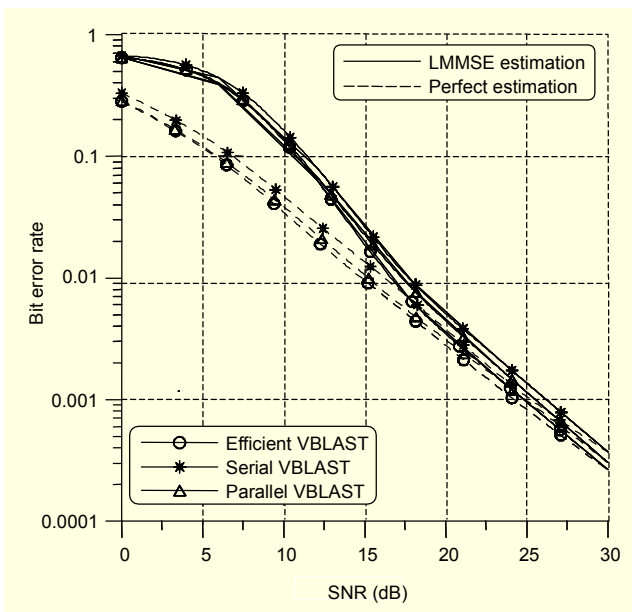


Fig. 5. BER performance of various OFDM-VBLAST detection schemes based on both perfect and LMMSE estimations in the case of  $N_t=2$  and  $N_r=2$ .

case of the exponential delay profile is negligible for some extra channel propagations. However, there is an irreducible MSE floor due to imperfect windowing for a relatively high SNR.

As for the channel estimation in the OFDM system with multiple antennas, some works formulated the training preamble sequences by minimizing the error covariance of the time-domain channel response [3], [4], which is basically similar to our approach. So, both approaches attain the same MSE bound [3]. If the condition of  $\lfloor K/L_t \rfloor \geq L$  is satisfied

and some parameters are suitably chosen, our approach in the time domain can give the same MSE performance bound to the above mentioned approaches. On the other hand, our approach is simpler for analysis than others [3], [4] because the channel estimation is simply done by only shifting by  $n_b$ , as we can see from (14) and (15).

Figures 5 and 6 show the evaluated bit error rate (BER) performances of both perfect and LMMSE channel estimations for the various VBLAST detection schemes of  $N_t=N_r=2$  and  $N_t=N_r=4$ . In Fig. 6, we can observe that the hybrid detection method provides improvements of approximately 2 dB and 7 dB over the classical methods with serial and parallel detection, respectively, when the required BER is  $10^{-3}$ . Also, it can be easily observed from the BER results of Figs. 5 and 6 that the performance of parallel detection is markedly better than that of classical VBLAST detection for  $N_t=2$ . In the case of  $N_t=3$ , however, its performance becomes worse. And the ordinary VBLAST based on serial and parallel detections requires  $N_t$  and  $2N_t$  nulling operations, respectively. The hybrid VBLAST detection scheme needs  $N_t(N_r+1)/2$  nulling operations, which results in additional complexity. On the other hand, the total number of rows used to obtain the pseudo-inverse matrix of  $\mathbf{H}_{k_i}$  is calculated as  $N_t(N_r+1)/2$ ,  $N_t(N_r+1)$  and  $N_t(N_r+1)(N_r+2)/6$  for serial, parallel and hybrid detection, respectively. In the case of  $N_t=N_r=4$ , for example, the total number of rows for hybrid detection is equal to that of parallel detection [7] and double that of sequential detection [2].

Figure 7 illustrates the effect of the number of transmitting antennas on the BER performance of the perfect estimation

with SNR as a parameter. As the number of transmitting antennas increases, as expected, the BER increases. Regardless of the number of transmitting antennas and SNR, the proposed hybrid detection scheme appears to be a stable tendency over other reference VBLAST systems [2], [7].

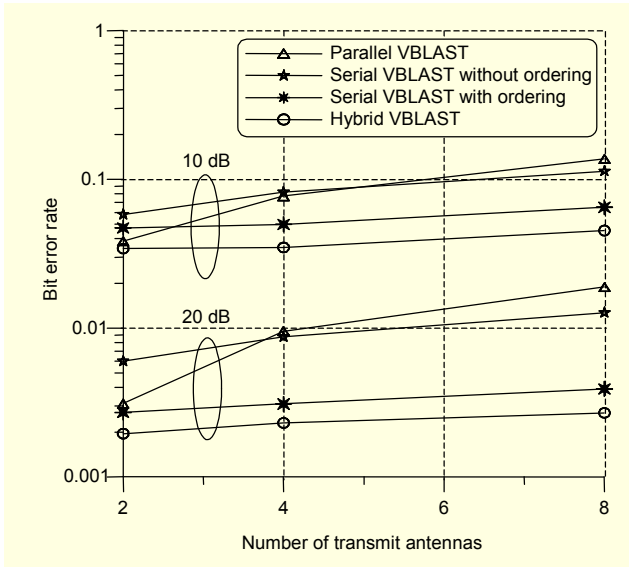


Fig. 7. BER performance of perfect estimations according to the number of transmitting antennas for various MIMO-VBLAST detection schemes.

## VIII. Conclusions

In this paper, OFDM with multiple transmitting and receiving antennas has been used to form an OFDM-based VBLAST system to increase system capacity. An efficient detection algorithm for a pilot symbol assisted interference nulling vector and cancellation has been studied for OFDM-based VBLAST systems. We have shown that the BER performance of hybrid detection outperforms ordinary OFDM-VBLAST based on serial and parallel detections at the expense of a small hardware complexity.

## References

- [1] G.J. Foschini, "Layered Space-Time Architecture for Wireless Communications in a Fading Environment When Using Multi-Element Antennas," *Bell System Technol. J.*, vol. 1, no. 2, Autumn 1996, pp. 41-59.
- [2] G.J. Foschini, G.D. Golden, R.A. Valenzuela, and P.W. Wolniansky, "Simplified Processing for High Spectral Efficiency Wireless Communication Employing Multi-Element Arrays," *IEEE J. Select. Areas Comm.*, vol. 11, no. 17, Nov. 1999, pp. 1841-1852.
- [3] E.G. Larsson and J. Li, "Preamble Design for Multiple-Antennas

- OFDM-Based WLANs with Null Subcarriers," *IEEE Signal Processing Lett.*, vol. 8, no. 11, Nov. 2001, pp. 258-288.
- [4] Y. (G) Li, "Simplified Channel Estimation for (OFDM) Systems with Multiple Transmit Antennas," *IEEE Trans. Wireless Comm.*, vol. 1, no. 1, Jan. 2002, pp. 67-75.
- [5] W.G. Jeon, K.H. Paik, and Y.S. Cho, "Two-Dimensional Pilot-Symbol-Aided Channel Estimation for OFDM System with Transmitter Diversity," *IEICE Trans. Comm.*, vol. E85-B, no. 4, Apr. 2002, pp. 840-844.
- [6] R.J. Piechocki, P.N. Fletcher, A.R. Nix, C.N. Canagarajah, and J.P. McGeehan, "Performance Evaluation of BLAST-OFDM Enhanced Hiperlan/2 Using Simulated and Measured Channel Data," *Electronics Lett.*, vol. 37, no. 18, Aug. 2001, pp. 1137-1139.
- [7] W.H. Chin, A.G. Constantinides, and D.B. Ward, "Parallel Multistage Detection for Multiple Antenna Wireless Systems," *Electronics Lett.*, vol. 38, no. 12, June 2002, pp. 597-599.
- [8] C. Elena, Qin Haiyan, Tao Xiaofeng, Yu Zhuizhuan, and Zhang Ping, "New Detection Algorithm of V-BLAST Space-Time Code," *Vehicular Technology Conf.*, vol. 4, 2001, pp. 2421-2423.
- [9] Zha Wei and S.D. Blostein, "Modified Decorrelating Decision-Feedback Detection of BLAST Space-Time System," *IEEE Int'l Conf. Comm.*, vol. 1, 2002, pp. 335-339.



**Yoon-Jae So** was born in Seoul, Korea, in 1976. He received the BS degree from Sejong University, Seoul, Korea, in 2002. He is currently with the Department of Information & Communications Engineering, Sejong University, Seoul, Korea. His research interests are in the areas of wireless communication systems design, signal processing and data communications.



**Hyoung-Goo Jeon** received the BS degree from Inha University, Incheon, Korea, in 1987 and the MS and Ph.D degrees from Yonsei University, Seoul, Korea, in 1992 and 2000, all in electronic engineering. From 1987 to 2000, he was with Electronic and Telecommunication Research Institute, Daejeon, Korea. Since 2001, he has been a Professor in the Information Communication Engineering Department of Dongeui University, Busan, Korea. His research interests include WLAN, CDMA modems and digital communications.



**Young-Hwan You** was born in Pochun, Korea, in 1970. He received the BS, MS, and PhD degrees in electronic engineering from Yonsei University, Seoul, Korea, in 1993, 1995, and 1999. From 1999 to 2002 he was a Managerial Engineer in Korea Electronics Technology Institute (KETI), Korea. Since 2002 he has been

an Assistant Professor of the Department of Internet Engineering, Sejong University, Seoul, Korea. His research interests are in the areas of wireless/wired communications systems design, spread spectrum transceivers, and systems architecture for realizing advanced digital communications systems, especially, for wireless personal area networks (WPAN).



**Myung-Sun Baek** was born in Seoul, Korea, in 1980. He received the BS degrees in information communications engineering from Sejong University, Seoul, Korea, in 2003. He is currently with the Department of Information Communications Engineering, Sejong University, Seoul, Korea. His research interests

are in the areas of wireless communication systems design, digital multimedia broadcasting (DMB), and data communications.



**Hyoung-Kyu Song** was born in Chungcheongbuk-do, Korea, on May 14, 1967. He received the BS, MS, and PhD degrees in electronic engineering from Yonsei University, Seoul, Korea, in 1990, 1992, and 1996. From 1996 to 2000 he was a Managerial Engineer in Korea Electronics Technology Institute (KETI), Korea.

Since 2000 he has been an Assistant Professor of the Department of Information and Communications Engineering, Sejong University, Seoul, Korea. His research interests include digital and data communications, information theory and their applications with an emphasis on mobile communications.